THE SHARED MOBILE ATMOSPHERIC RESEARCH AND TEACHING RADAR

A Collaboration to Enhance Research and Teaching

BY MICHAEL I. BIGGERSTAFF, LOUIS J. WICKER, JERRY GUYNES, CONRAD ZIEGLER, JERRY M. STRAKA, ERIK N. RASMUSSEN, ARTHUR DOGGETT IV, LARRY D. CAREY, JOHN L. SCHROEDER, AND CHRIS WEISS

Overcoming numerous challenges, a unique partnership created two C-band mobile Doppler weather radars capable of accurately measuring both clear-air circulations and damaging winds in heavy rain.

Starting with acquisition of two decommissioned 1974 C-band National Weather Service (NWS) Weather Surveillance Radars (WSR-74Cs) in early 1998, a coalition of scientists from the University of Oklahoma (OU), National Severe Storms Laboratory (NSSL), Texas A&M University (TAMU), and Texas Tech University (TTU) embarked on a project to build and deploy two mobile C-band Doppler weather radars for storm-scale research and to enhance graduate and undergraduate education in radar meteorology. This project culminated in the successful development and deployment of the first mobile C-band Doppler weather radar, dubbed SR-1, in 2001 (Fig. 1). To

FIG. 1. Side view of SR-1, the first mobile C-band Doppler weather radar in the United States. The smaller dish on top the cab is a self-pointing satellite-based Internet communication system that will allow for the real-time transmission of the data back to a remote server. Photo taken at NSSL where the SMART radars are housed. View is to the east-northeast.

AFFILIATIONS: BIGGERSTAFF AND STRAKA—School of Meteorology, University of Oklahoma, Norman, Oklahoma; WICKER AND ZIEGLER—National Severe Storms Laboratory, Norman, Oklahoma; GUYNES AND CAREY—Department of Atmospheric Sciences, Texas A&M University, College Station, Texas; RASMUSSEN—Cooperative Institute for Mesoscale Meteorological Studies, University of Oklahoma, Norman, Oklahoma; DOGGETT, SCHROEDER, AND WEISS—Department of Geosciences, Texas Tech University, Lubbock, Texas

CORRESPONDING AUTHOR: Dr. Michael Biggerstaff, School of Meteorology, University of Oklahoma, 100 E. Boyd Street, Room 1310, Norman, OK 73019-1013
E-mail: drdoppler@ou.edu
DOI:10.1175/BAMS-86-9-1263

In final form 25 January 2005

emphasize the collaborative nature and coownership of the radar facility, the system was named the Shared Mobile Atmospheric Research and Teaching (SMART) radar.

In this paper we discuss the rationale for building the mobile observing systems, highlight some of the challenges that were encountered in creating a multiagency coalition, provide examples of how the SMART radar is contributing to research and education, and discuss future plans for the continued development and management of the radar facility. Although the four institutions listed above jointly own the radars, other parties that are interested in using the facility may do so through collaboration with one of the four member institutions.

THE NEED FOR MOBILE OBSERVING SYSTEMS. Despite the enhanced observing opportunities afforded by the NWS Weather Surveillance Radar-1988 Doppler (WSR-88D) network (Crum and Alberty 1993; Crum et al. 1993), many basic physical processes and the internal dynamics of precipitating cloud systems remain poorly understood. In particular, phenomena like tornadogenesis (Lemon and Doswell 1979; Brandes 1984; Ziegler et al. 2001) and microbursts (Fujita 1981) that occur on short time and space scales (e.g., Wilson et al. 1984), or damaging straight-line winds from bow echoes (Johns 1993; Przybylinski 1995; Weisman 2001) that require observations of the low levels of the atmosphere, are generally not well sampled by the WSR-88D network. This is also true for infrequent events, like landfalling hurricanes (e.g., Powell et al. 1991). The development, testing, and refinement of hypotheses related to the physical processes associated with these phenomena require access to specialized datasets with temporal and spatial characteristics that match the fundamental scale of the process being examined.

To provide the bulk of the specialized radar data needed for fundamental research, the scientific community has, in the past, relied on either fixed-site deployable instrumentation or airborne observing systems. These two types of platforms have complimentary strengths and weaknesses. For example, a fixed-site ground-based instrument can operate continuously to provide rapid sampling of storm systems with particular emphasis on the lowest altitudes. Airborne platforms, however, require significant lead time for launch, cannot operate continuously, have longer times between samples of the same part of the storm (due to the time needed to turn the aircraft), and cannot sample the lowest altitudes of the atmosphere very well due to ground clutter contamination, attenuation, and/or flight altitude restrictions. The advantage of airborne platforms is that they offer tremendous range in pursuing interesting targets over a large operational domain and can operate over bodies of water. This increases the opportunity for sampling a particular phenomenon, expands research into oceanic environments, and allows for a greater portion of a storm's life cycle to be documented than that which can be obtained by a fixed-site instrument.

Mobile radar systems combine many of the strengths of the two traditional classes of observing platforms. They offer flexibility in deployment that extends the operational domain and increases the likelihood of sampling a particular type of event, yet they can also operate continuously with rapid sampling that emphasizes the lowest altitudes of a storm system. The utility of mobile Doppler radars for storm-scale research of rapidly evolving low-level circulations was most notably established during the Verification of the Origin of Rotation in Tornadoes Experiment (VORTEX; Rasmussen et al. 1994) that made use of the Doppler on Wheels (DoWs), developed by Wurman et al. (1997). The bulk design of the SMART radars (Table 1) is similar to the characteristics of the DoWs in many respects. However, the SMART radars use a C-band instead of an X-band transmitter. The lower C-band frequency reduces signal loss from attenuation (cf. Hildebrand et al. 1981) and improves the Nyquist (unambiguous) velocity that can be measured with the radar. The trade-off is that the C-band radars have a slightly larger beamwidth than the X-band radars for a given antenna size and, hence, offer less resolution for observing small-scale circulations. The SMART radars also have a modern digital signal processor that allows for flexibility in clutter rejection and improved signal quality.

The SMART radars were specifically designed to extend the range of atmospheric circulations that could be studied to include mesoscale systems (tens to hundreds of kilometers in horizontal scale) and to facilitate multiscale analysis when they are deployed in combination with existing ground-based observing systems. For example, during landfalling hurricanes the greater effective range of the C-band systems can be used to map inland flooding and diagnose changes in the mesoscale circulations within rainbands and the eyewall, while the X-band and higher-frequency radars focus on the structure of the individual elements and turbulence (including tornadoes) that are associated with the rainbands and eyewall. Such a combined multidimensional observational dataset is a requirement for data assimilation and model validation studies.

Table 1. SMART radar characteristics.	
Subsystem	**Description**
Platform	4700 International dual-cab diesel truck
Physical dimensions	length ~10 m (32 ft. 10 in.); height ~4.1 m (13 ft. 6 in.); weight ~11,800 kg total system
Power plant	10-kW diesel generator
Leveling system	Computer assisted; variable rate manual hydraulic controls
Transmitter	Frequency 5635 MHz (SR-1) 5612.82 MHz (SR-2)
Type	Magnetron; solid-state modulator and high-voltage power supply
Peak power	250 kW
Duty cycle	0.001
Pulse duration	Four predefined values selectable from 0.2 to 2.0 μs
Polarization	Linear horizontal
Antenna	Size 2.54-m diameter solid parabolic reflector
Gain	40 dB (estimated)
Half-power beam	Circular, 1.5° wide
Rotation rate	Selectable from 0–33 deg s^{-1}
Elevation range	Selectable from 0°–90°
Operational modes	Pointing, full PPI, range–height indicator (RHI), sector scans
Signal processor	SIGMET RxNet7 with AUX board
Maximum number of bins per ray	2048
Bin spacing	Selectable from 66.7 to 2000 m
Moments	Radar reflectivity (filtered and unfiltered), velocity, spectrum width
Ground clutter filter	seven user-selectable levels
Range averaging	Selectable
Dual-pulse repetition frequency dealiasing	Selectable
Processing modes	Pulse pair, fast Fourier transform, random phase
Data archive	CD-ROM; SIGMET IRIS format
Display	Real-time PPI; loop, pan, and zoom PPI or RHI products

COALITION MILESTONES. Progress toward developing the SMART radars began with acquisition of two decommissioned NWS WSR-74Cs in January 1998 by TAMU. Shortly thereafter, NSSL and OU offered the initial cash contributions for the development phase of the radar systems. A major financial boost to the project was provided by TTU during the first group meeting held at NSSL in March 1999. Rather than seek the remaining support from a single federal agency, it was decided that the coalition would instead develop the systems using internal funds. This decision allowed for flexibility in the system design but also added complexity in trying to ensure that each institution contributed somewhat equally to the project. Another distinct advantage to using internal funds was the ability to charge for the use of the equipment. The cost of maintenance of the equipment could then be paid directly by user fees collected by the member institutions from the project sponsors.

The coalition proceeded with ordering major components of hardware during the fall and winter of 1999. Work began on the radar pedestals and transmitters at TAMU (Fig. 2), while NSSL and OU

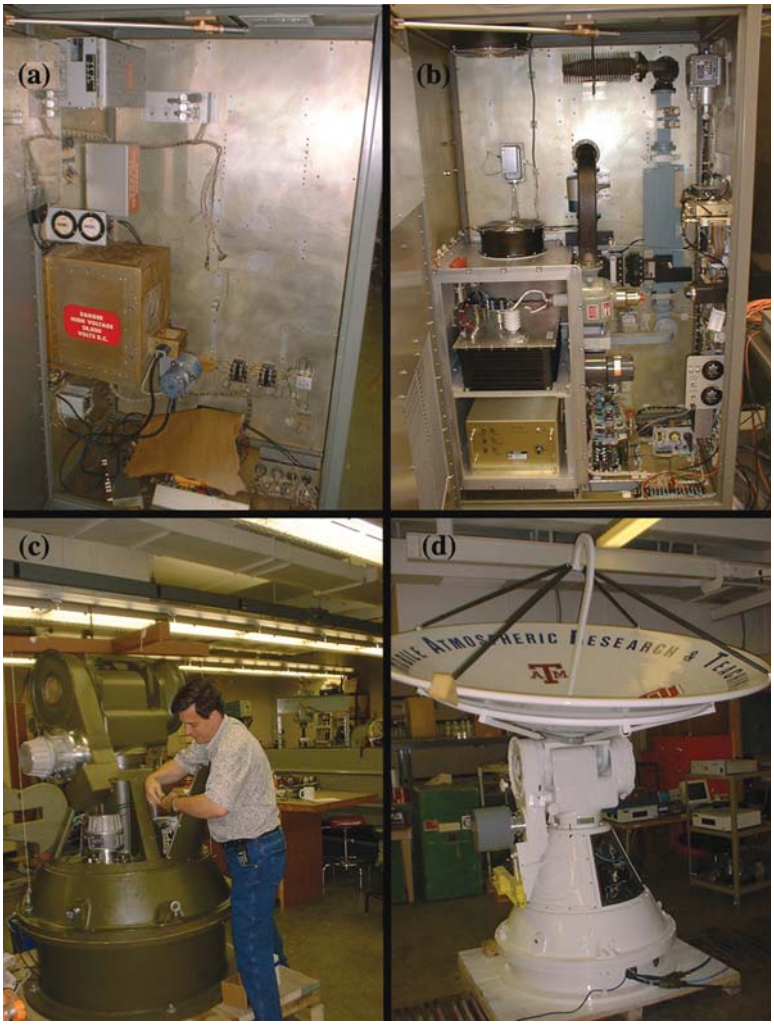

Fig. 2. Inside view of the SMART radar transmitter a) before and b) after modification. Note the a) original size of the high-voltage cage, identified by the red label, compared to b) the custom-fabricated unit in the lower-left portion of the transmitter cabinet. The high-voltage cage was increased in size by a factor of 2 to accommodate the new solid-state modulator and high-voltage power supply. c) The World War II era cast-iron pedestal was refurbished both mechanically and electrically at TAMU by J. Guynes (shown). d) The final product was repainted and integrated with the NWS WSR-74C antenna.

were securing, modifying, and outfitting the truck platforms (Fig. 3). In January 2001 a major modification was made to the transmitter design to improve the system reliability and performance by adding a solid-state modulator. This modification resulted in a significant increase in cost that was covered by additional contributions from OU and TAMU.

On 3 July 2001, a fire at a NSSL storage facility consumed one of the SMART radars (Fig. 4). This fire also destroyed most of NSSL's mobile instrumentation and a newly acquired three-dimensional lightning mapping system that was to be deployed that fall. Fortunately, there was no loss of life associated with the fire. With regard to the SMART radar project, only the truck, radar pedestal, and diesel generator were lost; the transmitter, antenna controller, and signal processor had not yet been installed on that unit. The recovery took time. The second SMART radar (SR-2) was finished and delivered on 12 May 2003, almost 2 yr after the completion of SR-1.

A memorandum of agreement (MOA) for how the systems would be managed was developed by the scientists and signed by all four institutions on 15 July 2002, with OU as the administrative center for the SMART radars.

CONTRIBUTIONS TO RESEARCH AND EDUCATION.

Research. The SR-1 has been deployed in several federally sponsored field campaigns. The first was the Keys Area Microphysics Project (KAMP), a part of the National Aeronautics and Space Administration's (NASA's) fourth Convection and Moisture Experiment (CAMEX-4). KAMP dealt with validating and improving the representation of microphysical processes in cloud resolving models that were used to perform retrievals of rain and latent heating from satellite-based passive microwave observations (cf. Kummerow et al. 2000; Biggerstaff et al. 2005, manuscript submitted to *J. Appl. Meteor.*; Seo and Biggerstaff 2005, manuscript submitted to *J. Appl. Meteor.*). More than 100 h of data were collected by SR-1 during KAMP, including 12 h of continuous coverage during the landfall of Tropical Storm Gabrielle on 14 September 2001 (Fig. 5; Knupp et al. 2005).

The National Science Foundation's (NSF's) International H2O Project (IHOP), conducted during spring 2002, was the second major field experiment in which SR-1 participated. Clear-air returns from the SMART radar during the interaction of a cold front, a dryline, and boundary layer rolls on 24 May 2002 reveal low-level convergence and upper-level divergence along the dryline (Fig. 6). Such vertical circulations in the presence of sufficient boundary

layer moisture often lead to the initiation of deep convection (Hane et al. 1993; Ziegler and Rasmussen 1998).

During fall 2002, SR-1 was used to study the structure of turbulent flows associated with landfalling hurricanes as part of a National Institute of Standards and Technology (NIST) project. The radar was deployed in both Hurricane Isidore and Hurricane Lili, and was used to relate radar-observed velocity perturbations to turbulence measured by a set of instrumented towers located near the radar site. The radar, located at Lafayette Municipal Airport in Lafayette, Louisiana (about 40 km inland), was subjected to wind gusts in excess of 36 m s^{-1}, but still collected data continuously (Fig. 7).

Additional hurricane experiments, sponsored by NASA and NSF, included the first dual–SMART radar deployment that occurred in September 2003 during the intercept of Hurricane Isabel. The two radars were separated by 50 km and collected more than 13 h of coordinated observations of the inner rainband and eyewall as the storm made landfall in North Carolina. The center of circulation passed

Fig. 3 (above right). a) The International 4700 truck had to undergo extensive modification, including b) the addition of a bed and hydraulics to allow leveling of the radar system. Once the platform was finished, c) overall integration was performed in the parking lot of the Eller Oceanography and Meteorology building on the campus of Texas A&M University.

Fig. 4 (right). A fire at the NSSL balloon barn on 3 Jul 2001 consumed one of the SMART radars during its construction phase. a) The cab melted and burned away, as did the tires. b) The truck was left resting on its hydraulic legs. c) The roof of the building collapsed and came to rest on the top of the radar pedestal. Both lead and aluminum metal parts melted in the fierce heat. d) (left) M. Biggerstaff and (right) J. Guynes along with L. Wicker and C. Ziegler (not shown) worked in the burned-out building to salvage custom-made components. Few parts were able to be reused.

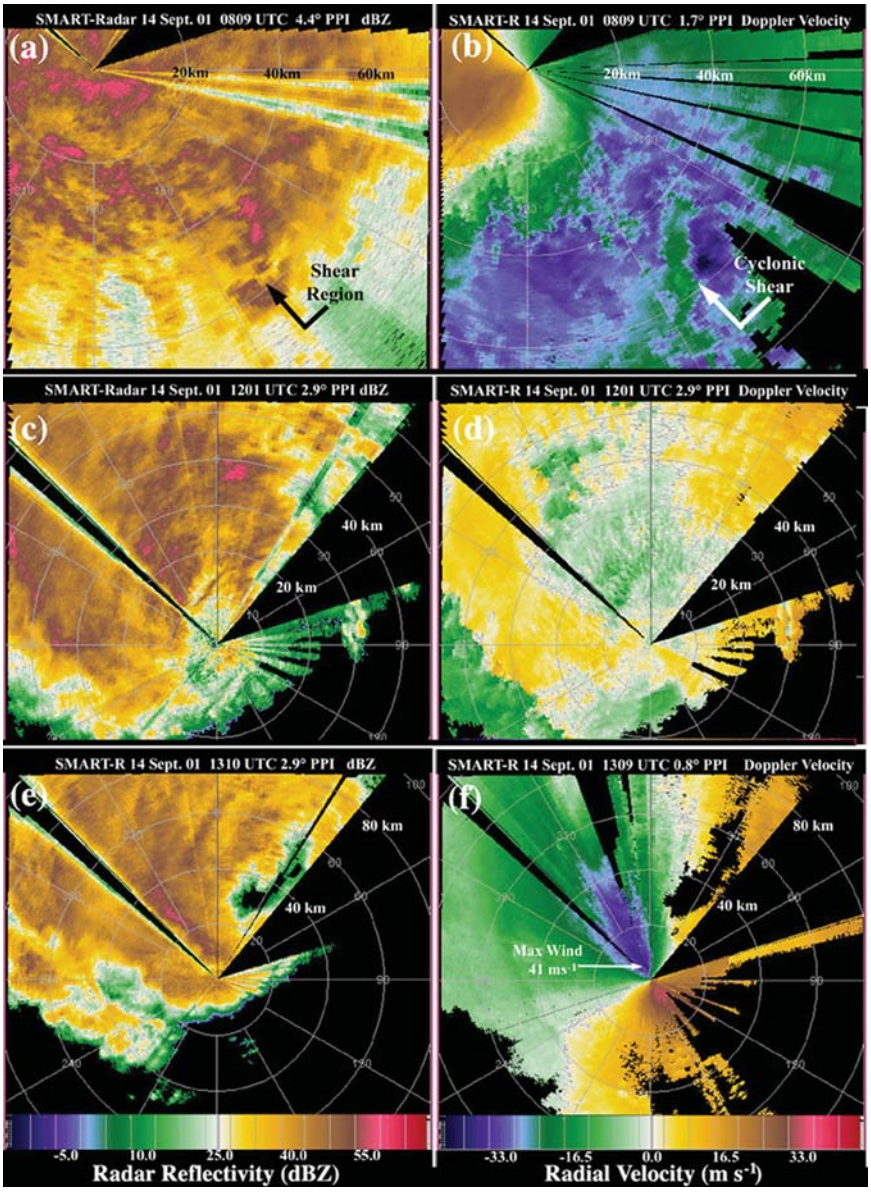

Fig. 5. a) Radar reflectivity (dBZ), according to the color scale at the lower-left portion of the figure, and b) Doppler velocity (m s^{-1}), according to the color scale in the lower-right portion of the figure with receding (approaching) flow indicated by positive (negative) values, taken by SR-1 during the landfall of Tropical Storm Gabrielle in Venice, FL, on 14 Sep 2001 during the time of a F0 tornado, indicated by the arrow pointing to the cyclonic shear in panel b). That was the first tornadic circulation observed by SR-1. Gabrielle formed c) a small eye just before d) the center of circulation made landfall at 1201 UTC as a rainband rotated around the southern portion of the vortex center. The strongest winds e) observed by SR-1 occurred in this rainband and were f) measured at 41 m s^{-1} at an altitude of about 200 m. The large pie-shaped wedge of missing data centered near 60° in the azimuth (toward the east-northeast) is a result of an optional software switch that automatically turns off the transmitter as the antenna sweeps through the angles subtended by the cab. This reduces exposure to microwave energy for the scientists operating the radar. Smaller wedges of missing data are the result of blockage by nearby trees.

through the region in which the Doppler data can be used to retrieve the three-dimensional flow, granting a unique opportunity to study circulations that contribute to inland flooding (Fig. 8). More recently, both SMART radars sampled the finescale turbulent structures in the airflow of Hurricane Frances as it slowly made landfall in Florida during 4–5 September 2004. In contrast to the stratiform nature of the inner band of Hurricane Isabel, the rainbands in Frances contained many convective elements that tested the operational limits of the SMART radars, with gusts in excess of 46 m s^{-1}.

While the original motivation for building the SMART radars was to facilitate storm-scale research, the clear-air capabilities of the systems have led to deployments in support of the U.S. Army's Homeland Security project in central Oklahoma. During spring 2003, the SMART radar collected data that were used to evaluate the potential for operational weather radars to detect simulated airborne releases of biological and chemical agents.

Also during spring 2003, NSSL and OU made use of SR-1 in the Cooperative Observational and Modeling Project for the Analysis of Severe Storms (COMPASS-03). Coordination with the DoWs and the University of Massachusetts's mobile X-band Doppler radar (Bluestein and Wakimoto 2003) was performed for a number of events, including the 10 May 2003 F3 tornado that passed through Oklahoma City, Oklahoma, and continued toward Tulsa, Oklahoma (Fig. 9). NSSL has taken the lead on using these observations for data assimilation experiments.

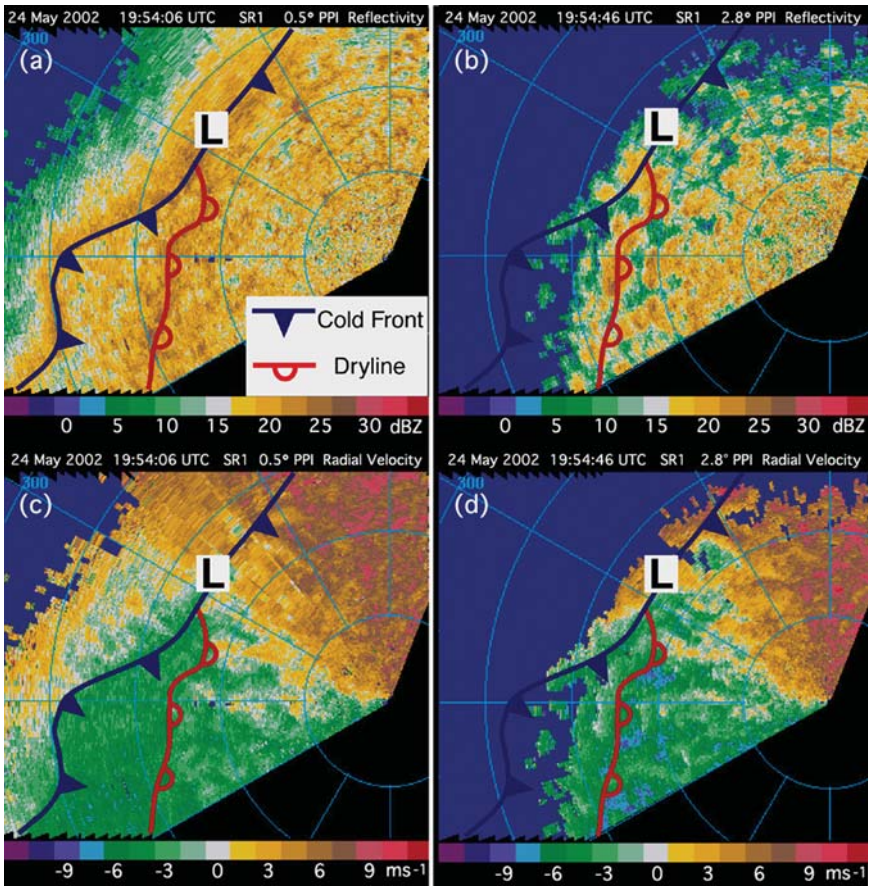

Fig. 6. The clear-air capability of the SMART radar is illustrated by this intersection of a nonprecipitating cold front and a dryline in Oklahoma during 24 May 2002. Range rings are every 10 km. a) The low-level reflectivity (dBZ), according to the color scale, clearly identifies the finescale structure of the frontal system, denoted by the inserted key, while b) the upper-level reflectivity shows a region of open cellular convection in the warm, moist air ahead of the dryline. The "L" marks the position of a subsynoptic low pressure center. c) The dryline is also marked by low-level convergence as shown by the 0.5° PPI Doppler velocity (m s^{-1}), according to the color scale with receding (approaching) flow indicated by positive (negative) values. For this color scale, white or yellow velocities followed in range along the same radial by green velocities indicate convergence. Several centers of convergence can be found at the leading edge of the dryline. d) At higher elevation angles, organized bands of velocity perturbations can be seen to be oriented quasi perpendicularly to the dryline. These mark the boundary layer rolls.

Tornadic storms were also sampled during the NSF-sponsored second Thunderstorm Electrification Experiment (TELEX-2). Both SMART radars were used in conjunction with the NSSL polarimetric S-band radar and a three-dimensional lightning mapping system to examine the relationship between cloud electrification and the evolution of airflow through convective storm systems over central Oklahoma. One storm, a cyclic supercell thunderstorm that was observed during TELEX-2, produced a tornado near Geary, Oklahoma, on 29 May 2004. Coordinated volume scans were obtained every 2.5 min for approximately 90 min as the storm moved across the region over which the three-dimensional winds could be retrieved. Combined with the three-dimensional lightning mapping array data, this represents an unprecedented set of observations for studying the relationship between airflow and the distribution and frequency of lightning in a tornadic supercell thunderstorm.

Immediately following TELEX-2, SR-1 participated in the Salt River Project's study of heavy rains and damaging microbursts during the southwestern monsoon over Arizona. Several convective systems were sampled, including one that produced a downdraft haboob (Fig. 10).

Education. One of the challenges in any university environment is obtaining access to state-of-the-art research tools for use in educational activities. Both graduate and undergraduate students have used the SMART radar during sponsored research projects. Such activities provide students with an opportunity to learn about the engineering aspects of radar meteorology, including system design, performance trade-offs, and the impact of signal processing on data quality and resolution. Students also learn how to optimize data collection in support of specific scientific objectives and how to interpret the radar data in real time.

To extend educational opportunities beyond sponsored research projects, the SMART radar MOA was designed to facilitate instruction and educational outreach by offering a reduced teaching use fee, com-

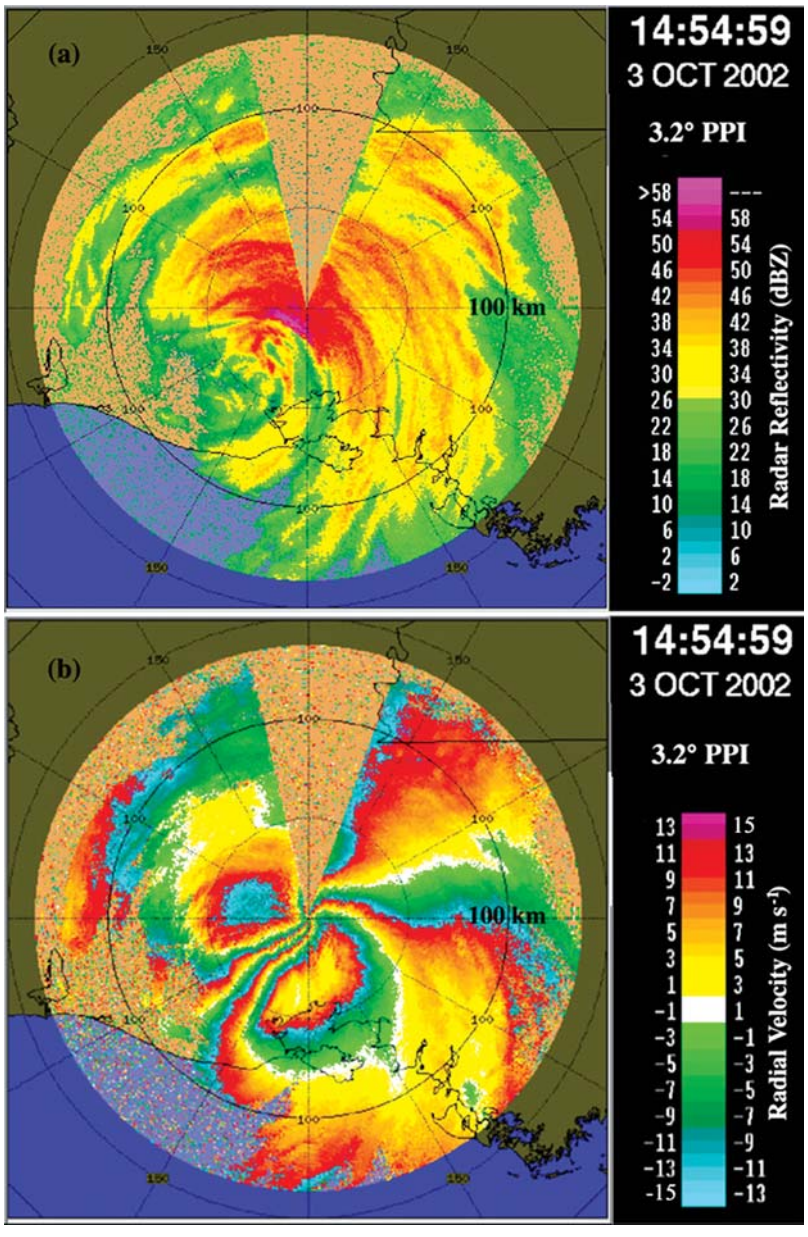

mensurate with student fees, collected in laboratory courses at most major universities. The School of Meteorology at OU sponsors access to the SMART radars as a laboratory for formal undergraduate and graduate radar meteorology courses. During the summers of 2003 and 2004, more than 40 sessions were conducted from 2200 to 0100 LT to provide small student groups with the opportunity for gaining experience operating the weather radar. More than 70 students participated.

The SMART radar has also been used to support informal university-level instruction and K–12 outreach. These included presentations to the Texas A&M and University of Oklahoma stu-

FIG. 7 (LEFT). Large-scale view of the a) raw radar reflectivity (dBZ), according to the color scale, and b) unedited Doppler velocity (m s^{-1}), according to the color scale with receding (approaching) flow indicated by positive (negative) values, during the landfall of Hurricane Lili in central Louisiana during 3 Oct 2002. Range rings are every 50 km. The unambiguous velocity was –15 m s^{-1}. Note that the C-band radar energy was able to penetrate through more than 100 km of moderately heavy to heavy rainfall. The reduced attenuation at the C band, relative to that found at the X band, was the key factor in our decision to use the C band for the SMART radars. The large pie-shaped wedge of missing data centered near 0° in the azimuth (toward the north) is a result of an optional software switch that automatically turns off the transmitter as the antenna sweeps through the angles subtended by the cab. This reduces exposure to microwave energy for the scientists operating the radar.

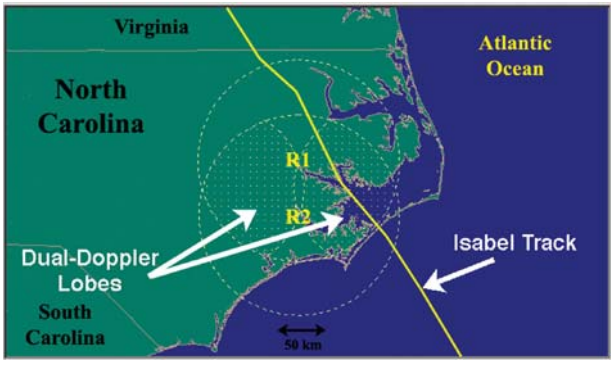

FIG. 8 (RIGHT). Map showing the track of Hurricane Isabel (denoted by the yellow line) relative to the location of SR-1 (denoted by R1) and SR-2 (denoted by R2) during the landfall that occurred on 18 Sep 2003. The dashed circles show the 100-km operational range of the radars during this deployment. Hatched regions, labeled as the dual-Doppler lobes, indicate the area over which the Doppler data from the two radars can be used to retrieve the three-dimensional wind. Note that the center of circulation of the hurricane passed through the middle of the easternmost dual-Doppler lobe.

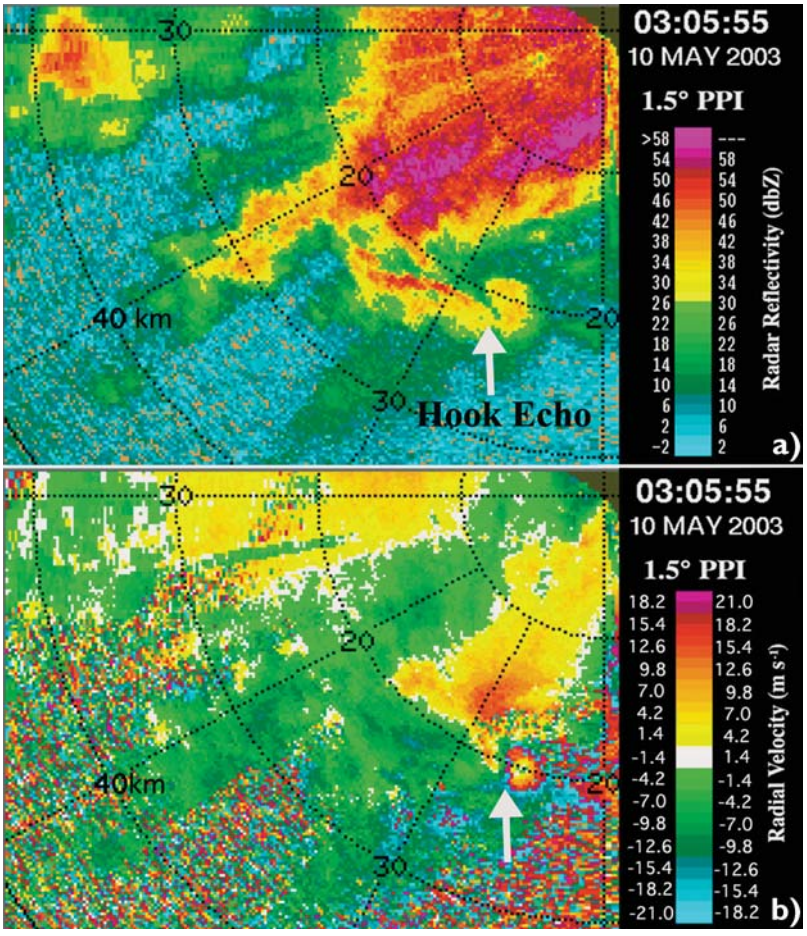

Fig. 9. Magnified view of a) raw radar reflectivity (dBZ), according to the color scale, and b) unedited Doppler velocity (m s^{-1}), according to the color scale with receding (approaching) flow indicated by positive (negative) values, during the 10 May 2003 F3 tornado that crossed Oklahoma City, OK. At this time the tornado was producing F1 damage. Range rings are every 10 km. The unambiguous velocity was –21 m s^{-1}. Note the large hook echo centered at the 22-km range and 210° in the azimuth in a) and the aliased approaching velocities denoted by the arrow in b) marking the tornado vortex at the 20-km range and 195° in the azimuth. The SMART radar was able to observe this tornadic circulation despite the ~15 km swath of very high radar reflectivity between the radar and the tornado. The reduced attenuation at the C band, relative to that observed at the X band, allows us to set the SMART radar ahead of the storm and collect data continuously as the storm approaches. A radar using an X-band transmitter would have to "chase" the storm from the southwest to avoid signal loss through the heavy rain and hail on the northern side of the storm system.

Fig. 10. Photograph (courtesy of K. Howard, NSSL) of SR-1 just ahead of a downdraft haboob (a strong dust storm) during the Salt River Project near Phoenix, AZ. The SMART radars have operated in environments ranging from 43° to –5°C in temperature, and from 20% to 100% in relative humidity, heavy rains, and winds in excess of 45 m s^{-1}.

dent chapters of the American Meteorological Society (Fig. 11), and hands-on demonstrations to more than 200 junior-high and high school students during the Oklahoma Climate Survey's Meteorological Science Fair held at OU during March 2003 and February 2004. The SMART radars also participated in a severe weather and storm awareness program at Cleveland Elementary School in Norman, Oklahoma, during April 2004. About 70 first-grade students completed a 90-min exercise on tornado safety facts, the ingredients that are necessary for tornadic storms, and how scientists use special tools like the SMART radars to study the atmosphere. Each student was allowed to sit in the operator's chair and control the antenna while a preprogrammed loop of the 10 May 2003 Oklahoma City tornado played on the monitor.

Community outreach, aimed at promoting science and engineering, is another facet of the SMART radar program. More than 300 people have been given demonstrations of the radars during visits to NSSL and OU. Recently, volunteers, ranging in age from 7 to 70 yr old, rode with the SMART radars during the Norman Christmas parade and distributed over 1000 candy canes to eager youngsters (Fig. 12).

Fig. 11. M. Biggerstaff, facing the camera, gives a demonstration of SR-1 to the Texas A&M student chapter of the American Meteorological Society in which he served as faulty advisor during the construction phase of the SMART radars. Similar demonstrations have been given to a number of organizations. Education and outreach is an important component of the SMART radar program.

Fig. 12. Photograph (courtesy of D. Schultz, NSSL) of SR-1 followed by SR-2 traveling down Main Street during the Norman, OK, Christmas parade on 11 Dec 2004. Several thousand spectators cheered and waved as volunteers, many from the OU student chapter of the American Meteorological Society, distributed candy canes to children lining the street. Participation in community events helps build good relations with the public, and promotes science and engineering.

FUTURE PLANS. *Hardware modifications.* Two key upgrades to the SMART radars are envisioned. The first is a joint project between NSSL and OU to install a broadband self-pointing satellite-based Internet communication system on SR-1 to facilitate the real-time transmission of the radar data (Fig. 1). In a preliminary test, data from an onboard personal computer that is networked to the radar signal processor has been passed through the satellite link to a remote server on the Internet. This test has shown that the system can achieve an average transfer rate that is sufficient for transferring compressed data files.

The goal of this project is to make the SMART radar data available with minimal delay through the World Wide Web, as well as through the Advanced Weather Interactive Processing System (AWIPS), to assist in severe storm warnings. This addresses one of the recommendations made by the National Research Council in their 2002 report, "Weather radar technology beyond NEXRAD."

The second upgrade is being led by OU in partnership with NSSL and involves adding polarization diversity to SR-2. This enhancement will extend research to include cloud microphysics (e.g., Straka et al. 2000) and quantitative precipitation estimation.

Field campaigns. Members of the SMART radar coalition are pursuing four major field campaigns. During winter 2005, NSSL will take SR-2 to southwestern Arizona for a follow-up on the Salt River Project, and then to the Great Lakes for a study of lake-effect snowbands. To investigate sources and movement of the lower-tropospheric ozone, TAMU will take finescale measurements of the airflow around Houston, Texas, during high-ozone-concentration events in a study sponsored by the Texas Commission on Environmental Quality (TCEQ). That project will employ both SMART radars from May through September 2005. TTU and OU are collaborating on proposals targeting landfalling tropical cyclones during 2006–07. Their objectives include diagnosing the structure and changes of turbulence in the hurricane boundary layer, the evolution of convection and damaging winds, inland flooding, and the transition to or interaction with extratropical cyclones. Also, OU is collaborating with NSSL on the next Verification of the Origin of Rotation in Tornadoes Experiment (VORTEX)-2 in which the two SMART radars will be complimented with a mobile X-band polarimetric radar, which is currently under development, to study storm-scale processes that lead to tornadogenesis.

It is important to note that even if all of the proposals are successful, the radars would still sit idle more than one-half of the time. Clearly, there are opportunities for other groups to make use of the systems.

METHOD OF COLLABORATION. Third parties that are interested in using the SMART radars should start by contacting the lead author, who is serving as director of the SMART radar program and maintains a schedule of planned activities for the

platforms. Normally the SMART radars are allocated on a quarterly basis, with each institution receiving seasonal access that rotates through the annual cycle over a 4-yr period. It is understood that the boundaries of the quarters are not rigid. Moreover, member institutions are allowed to trade or share quarters.

If the radars are available during the period of interest, a formal MOA can be established that transfers liability to the appropriate agency for the duration of the project. Experience suggests that 6 months may be needed to secure an agreement. The requesting institution must also pay a two-part use fee. The first part—a flat charge for access to the equipment—must be paid before the beginning of the project. The second part—an hourly use fee—is billed after the project has been completed. Even the institutions owning the equipment are required to pay these fees. A 3-day specialized training seminar held in Norman is also mandatory for all third-party users of the equipment.

Fees are used to help maintain the SMART radars and also to provide users with support from an engineering consultant to help troubleshoot any problems that may arise during a field experiment. Special arrangements may be made for additional support in collecting and/or quality controlling the data.

DATA ARCHIVE POLICY. Major field experiments often have an established data archive. For instance, the SMART radar data that were collected during KAMP are archived at Marshall Space Flight Center in Huntsville, Alabama. Similarly, the SMART radar data from IHOP are archived at the NSSL. For smaller field campaigns, data are generally archived by the principal investigator overseeing the instrument. For the SMART radar program, two copies of data are archived onto either CD-ROM or DVD disks at the end of each data collection shift. Within 3 months of the conclusion of a project one copy of the raw data is sent to NSSL for long-term storage.

Access to data collected by third-party users will follow the policies established by the funding agency that paid for the SMART radar deployment. For data collected by member institutions, outside parties may request copies of raw data on a cost-recovery basis from NSSL two years after the data were received.

Unfortunately, none of the member institutions are funded to maintain a long-term archive or to provide support to outside users. It would be best to obtain access to the data through collaboration with the SMART radar investigator that is responsible for its collection.

CONCLUSIONS. With successful completion of the first coordinated deployment of the two Shared Mobile Atmospheric Research and Teaching (SMART) radars during the landfall of Hurricane Isabel in North Carolina, the SMART radar coalition met its goal of developing and using two mobile C-band Doppler radars for storm-scale research. Both instruments proved to be effective in obtaining high temporal and spatial resolution data over mesoscale domains in storm systems that contained extreme winds and heavy rain. In addition to hurricanes, the C-band SMART radars have also demonstrated their effectiveness in studies of tornadic supercells, ordinary multicellular convective systems, boundary layer rolls, drylines, and clear-air convergence zones, and for detecting simulated releases of biological and chemical agents. Repeated successful intercepts provide evidence that these radars are capable of being used to study a wide range of atmospheric phenomena.

Upgrades that are currently underway to the radars will enable the real-time transmission of the data over the World Wide Web and into the National Weather Service Forecast Offices. Future plans also include adding polarimetric diversity to one of the platforms to enable further research in quantitative precipitation estimates, cloud physics, and cloud electrification.

In spring 2004, we used the radars in support of the Norman Public School District's Severe Weather Awareness Program at one of the elementary schools near the University of Oklahoma, and also demonstrated the radars during the Oklahoma Climate Survey's Meteorological Science Fair. Activities such as these illustrate how research-quality instrumentation can be used outside of the traditional university classroom to promote and stimulate scientific interest. Combined with frequent use of the radars for university instruction, the goal of enhancing meteorological education is being met. It is the intention of the coalition to continue to make the platforms available for education and outreach.

Collaboration with other scientists is another important goal of this program. The MOA that formed the SMART radar coalition encourages third-party use of the equipment. While this option has not yet been fully exercised, it is our sincere desire to see the SMART radars contribute to as many external programs as possible.

ACKNOWLEDGMENTS. Construction of the SMART radars was financed by the Office of the Vice President for Research at the University of Oklahoma (OU), Texas A&M

University (TAMU), and Texas Tech University (TTU), and the Director's Discretionary Fund at the National Severe Storms Laboratory (NSSL). Additional support was provided by the Cooperative Institute for Mesoscale Meteorological Studies and the School of Meteorology at OU, the Department of Atmospheric Sciences and College of Geosciences at TAMU, and the Wind Engineering Program at TTU. The coalition is grateful to J. Keeler and D. Carlson at the National Center for Atmospheric Research and J. Wurman at the Center for Severe Storms Research for guidance given during the incipient stages of the program.

SMART radar deployments that are discussed in this article were sponsored by the National Aeronautics and Space Administration under grants NAG5-11013 and NAG5-13262, the National Science Foundation under grants ATM-0130316 and ATM-01314188, the National Institute for Standards and Technology under cooperative award 70NANB8H0059, the National Oceanic and Atmospheric Administration's United States Weather Research Program and National Severe Storms Laboratory, and the U.S. Army.

REFERENCES

Bluestein, H. B., and R. M. Wakimoto, 2003: Mobile radar observations of severe convective storms. *Radar and Atmospheric Science: A Collection of Essays in Honor of David Atlas, Meteor. Monogr.,* No. 52, Amer. Meteor. Soc., 105–136.

Brandes, E. A., 1984: Vertical vorticity generation and mesocyclone sustenance in tornadic thunderstorms: The observational evidence. *Mon. Wea. Rev.,* **112,** 2253–2269.

Crum, T. D., and R. L. Alberty, 1993: The WSR-88D and the WSR-88D operational support facility. *Bull. Amer. Meteor. Soc.,* **74,** 1669–1688.

——, ——, and D. W. Burgess, 1993: Recording, archiving, and using WSR-88D data. *Bull. Amer. Meteor. Soc.,* **74,** 645–788.

Fujita, T. T., 1981: Tornadoes and downbursts in the context of generalized planetary scales. *J. Atmos. Sci.,* **38,** 1511–1534.

Hane, C. E., C. L. Ziegler, and H. B. Bluestein, 1993: Investigation of the dryline and convective storms initiated along the dryline: Field experiments during COPS-91. *Bull. Amer. Meteor. Soc.,* **74,** 2133–2145.

Hildebrand, P. H., R. A. Oye, and R. E. Carbone, 1981: X-band vs. C-band aircraft radar: The relative effects of beamwidth and attenuation in severe storm situations. *J. Appl. Meteor.,* **20,** 1353–1361.

Johns, R. H., 1993: Meteorological conditions associated with bow echo development in convective storms. *Wea. Forecasting,* **8,** 294–300.

Knupp, K. R., J. Walter, and M. I. Biggerstaff, 2005: Doppler profiler and radar observations of boundary layer variability during the landfall of Tropical Storm Gabrielle. *J. Atmos. Sci.,* in press.

Kummerow, C., and Coauthors, 2000: The status of the Tropical Rainfall Measuring Mission (TRMM) after two years in orbit. *J. Appl. Meteor.,* **39,** 1965–1982.

Lemon, L. R., and C. A. Doswell, 1979: Severe thunderstorm evolution and mesocyclone structure as related to tornadogenesis. *Mon. Wea. Rev.,* **107,** 1184–1197.

Powell, M. D., P. P. Dodge, and M. L. Black, 1991: The landfall of Hurricane Hugo in the Carolinas: Surface wind distribution. *Wea. Forecasting,* **6,** 379–399.

Przybylinski, R. W., 1995: The bow echo: Observations, numerical simulations, and severe weather detection methods. *Wea. Forecasting,* **10,** 203–218.

Rasmussen, E. N., R. Davies-Jones, C. A. Doswell, F. H. Carr, M. D. Eilts, D. R. MacGorman, and J. M. Straka, 1994: Verification of the Origins of Rotation in Tornadoes Experiment: VORTEX. *Bull. Amer. Meteor. Soc.,* **75,** 995–1006.

Straka, J. M., D. S. Zrnic, and A. V. Ryzhkov, 2000: Bulk hydrometeor classification and quantification using polarimetric radar data: Synthesis of relations. *J. Appl. Meteor.,* **39,** 1341–1372.

Weisman, M. L., 2001: Bow echoes: A Tribute to T. T. Fujita. *Bull. Amer. Meteor. Soc.,* **82,** 97–116.

Wilson, J. W., R. D. Roberts, C. Kessinger, and J. McCarthy, 1984: Microburst wind structure and evaluation of Doppler radar for airport wind shear detection. *J. Climate Appl. Meteor.,* **23,** 898–915.

Wurman, J., J. Straka, E. Rasmussen, M. Randall, and Z. Zahrai, 1997: Design and deployment of a portable pencil-beam, pulsed, 3-cm Doppler radar. *J. Atmos. Oceanic Technol.,* **14,** 1502–1512.

Ziegler, C. L., and E. N. Rasmussen, 1998: The initiation of moist convection at the dryline: Foreasting issues from a case study perspective. *Wea. Forecasting,* **13,** 1106–1131.

——, ——, T. R. Shepherd, A. I. Watson, and J. M. Straka, 2001: The evolution of low-level rotation in the 29 May 1994 Newcastle–Graham, Texas, storm complex during VORTEX. *Mon. Wea. Rev.,* **129,** 1339–1368.